

# High fidelity blazed grating replication using nanoimprint lithography

Chih-Hao Chang,<sup>a)</sup> J. C. Montoya, M. Akilian, A. Lapsa,  
R. K. Heilmann, and M. L. Schattenburg

*Space Nanotechnology Laboratory, Massachusetts Institute of Technology, Cambridge, Massachusetts 02139*

M. Li

*Nanonex Corporation, 1 Deer Park Drive, Suite O, Monmouth Junction, New Jersey 08852*

K. A. Flanagan

*Center for Space Research, Massachusetts Institute of Technology, Cambridge, Massachusetts 02139*

A. P. Rasmussen

*Columbia Astrophysics Lab, 550 West 120th Street, New York, New York 10027*

J. F. Seely and J. M. Laming

*Naval Research Laboratory, Space Science Division, Washington, DC 20375*

B. Kjornrattanawanich

*Universities Space Research Association, Brookhaven National Laboratory, Upton, New York 11973*

L. I. Goray

*International Intellectual Group, Inc., Penfield, New York 14526*

(Received 14 June 2004; accepted 30 August 2004; published 13 December 2004)

We report progress in using nanoimprint lithography to fabricate high fidelity blazed diffraction gratings. Anisotropically etched silicon gratings with 200 nm period and 7.5° blaze angle were successfully replicated onto 100 mm diameter wafers with subnanometer roughness and excellent profile conformity. Out-of-plane distortion induced by residual stress from polymer films was also analyzed and found to be extremely low. The replicated blazed gratings were tested and demonstrated high x-ray diffraction efficiencies. This process was developed for fabricating blazed diffraction gratings for the NASA *Constellation-X* x-ray telescope. © 2004 American Vacuum Society. [DOI: 10.1116/1.1809614]

## I. INTRODUCTION

Blazed diffraction gratings are important in a number of applications, due to their ability to maximize diffraction efficiency at the specular reflection angle off the blazed facets. For applications in x-ray spectroscopy, it is essential to use blazed diffraction gratings to achieve high efficiency grazing-incidence reflection. Fabrication of blazed gratings has been thoroughly explored, yet previous methods have disadvantages including poor blaze profile, high surface roughness, and low throughput.<sup>1-3</sup> For NASA's x-ray telescope *Constellation-X*, a total grating area on the order of 100 square meters is required.<sup>4,5</sup> Thus a cost and time efficient process to fabricate thousands of high fidelity blazed gratings is desirable.

In previous efforts,<sup>6</sup> we reported replicating saw-tooth profile gratings using nanoimprint lithography (NIL).<sup>7,8</sup> Preliminary imprint results from 400 nm period inverted triangular gratings and 200 nm period gratings with 7.5° blaze were reported. The imprinted blazed polymer gratings demonstrated x-ray diffraction efficiencies that are comparable to those of the silicon master.<sup>9</sup> However, several factors have limited the performance of the imprinted gratings. The residual layer was not properly controlled in the imprinting

setup, resulting in relatively thick films. The separation mechanism was also not ideal, which may have partly been the cause of groove edge rounding.

In a collaboration with Nanonex Corporation, those limiting factors were better controlled in a commercially ready NIL system. Using both thermal-cure and ultraviolet (UV)-cure processes, 200 nm period gratings with 7.5° blaze were imprinted onto 100 mm diameter wafers. The imprinted polymer gratings show high profile conformity and improved x-ray diffraction efficiencies.

Possible out-of-plane distortion of the wafer induced by residual polymer film stress was also analyzed. In some applications, the out-of-plane distortion needs to be tightly controlled. For example, the flatness of the x-ray diffraction gratings used for *Constellation-X* will need to be less than 0.5 μm across 100 mm. Using a Shack-Hartmann wave front metrology setup<sup>10</sup> the surface profile of the wafers before and after imprinting was characterized to analyze the effect of the polymer imprint film.

## II. BLAZED GRATING FABRICATION AND REPLICATION

The blazed grating used as the master was fabricated using an off-cut silicon wafer with its wafer normal rotated 7.5° from the [111] direction along the [1 $\bar{1}$ 0] axis.<sup>6</sup> The 200 nm period grating lines were patterned using an interfer-

<sup>a)</sup>Electronic mail: chichang@mit.edu

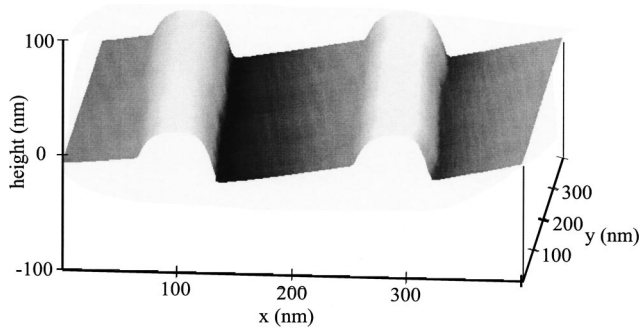


FIG. 1. AFM image of anisotropically etched 200 nm period silicon grating with 7.5° blaze. The round top and sharp bottom edges are AFM artifacts.

ence lithography setup. The pattern was transferred using reactive ion etching to a silicon nitride layer, which was used as the mask for the subsequential anisotropic KOH etch. The nitride mask was removed with HF. The resulting atomic force micrograph (AFM) can be seen in Fig. 1. The reentrant profile of the blazed grating is problematic for probe based metrology tools to image and thus creates artifacts. The root-mean-square (rms) roughness of the blazed facets as measured by AFM is  $<0.2$  nm.

The replication of the blazed gratings was conducted at Nanonex Corporation. The NX-1000 nanoimprinter was used for the thermal-cure process, with NXR-1020 as the imprint resist. The blazed grating was imprinted onto a 100 mm diameter silicon wafer at a temperature of 120 °C and pressure of 200 psi. AFM and scanning electron microscope (SEM) images of the imprinted gratings are shown in Fig. 2. The rms roughness of the blazed facets is  $<0.2$  nm.

The NX-2000 nanoimprinter was used for the UV-cure process, with NXR-2010 as the imprint resist and NXR-3020 as the underlying layer ( $\sim 200$  nm). The underlying layer is typically used for planarization and pattern transfer. The underlying layer is not essential to our application, and was used only because it is a standard process for UV-cure NIL.<sup>11</sup> The blazed grating was cured over a 100 mm diameter fused silica wafer with a dose of 250 mJ/cm<sup>2</sup> at room temperature and a pressure of 80 psi. A more detailed description of both imprint processes is outlined in Li *et al.*<sup>11</sup> An AFM image of the imprinted grating is shown in Fig. 3. The rms roughness of the blazed facets is  $<0.2$  nm.

### III. OUT-OF-PLANE DISTORTION

Out-of-plane distortion of a wafer will occur due to the residual stress of the deposited thin film.<sup>12</sup> Residual stress might be thermal stress, due to thermal mismatch between the wafer and polymer film during the thermal cycle, or intrinsic stress, which results when the polymer crosslinks or changes state. For applications where extremely flat optics are used, large out-of-plane distortion induced during the fabrication process might lead to significant design errors. Thus the change of wafer flatness due to the NIL process was analyzed.

Using a Shack–Hartmann (S–H) wave front metrology tool the surface profile of a wafer can be mapped. By map-

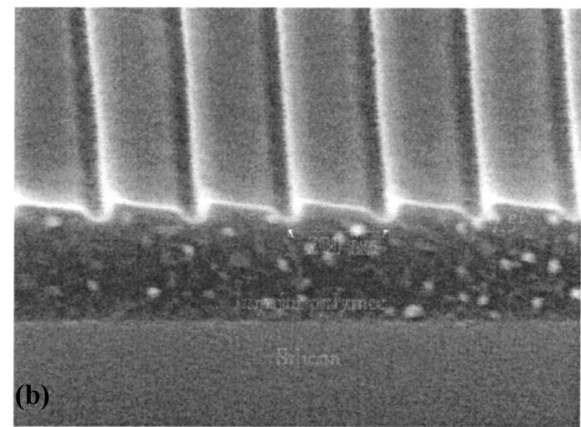
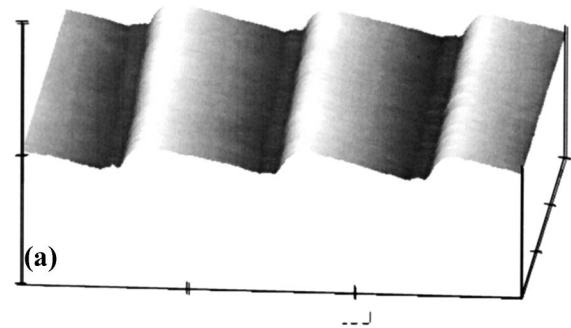


FIG. 2. Images of imprinted blazed grating using thermal-cure process, (a) AFM, (b) cross-section SEM.

ping the back surface of the wafer before and after imprinting, the out-of-plane distortion due to the NIL process can be characterized. The backwafer surface profile before and after imprinting can be seen in Fig. 4 for the thermal-cure process and Fig. 5 for the UV-cure process. The average polymer layer thickness for these experiments is around 85 nm for the thermal-cure process and 285 nm for the UV-cure process, as measured by cross-section SEM.

For both imprint processes the surface profile of each wafer does not undergo any apparent change. The surface profile was reconstructed using a least-squared fit algorithm of the slope field to Zernike polynomials.<sup>13</sup> The Zernike coefficients can be examined to yield a more accurate conclusion, since the effects of tip and tilt can be subtracted. The Zernike

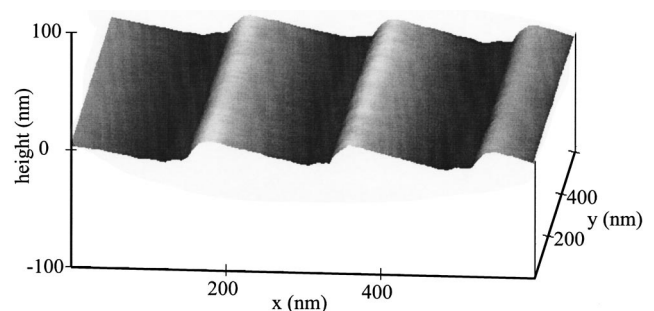
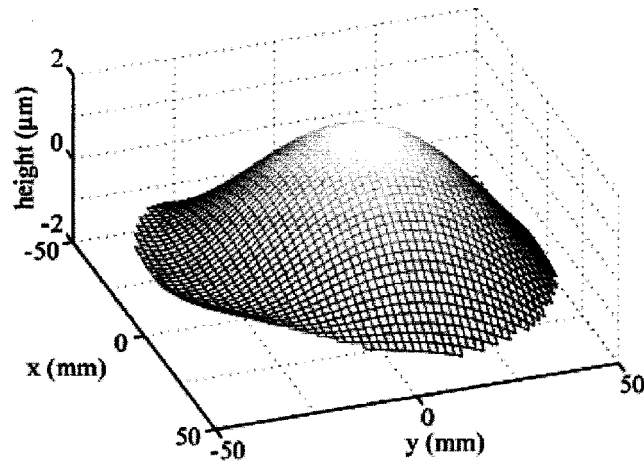
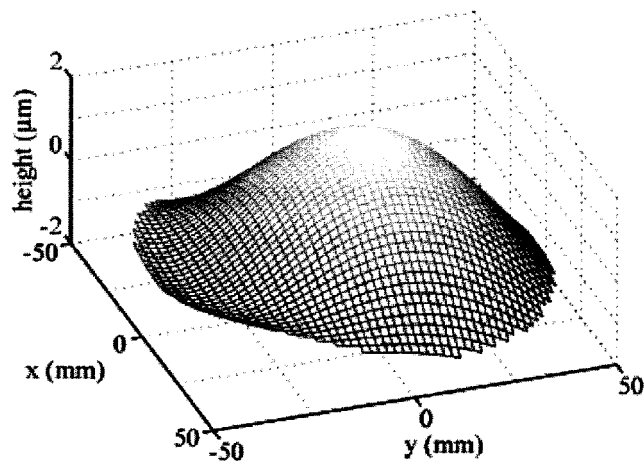


FIG. 3. AFM image of imprinted blazed grating using UV-cure process.



(a)



(b)

FIG. 4. Wafer backsurface profile (a) before, and (b) after the thermal-cure imprint process. The peak-to-valley surface topography value changes from 3.601 to 3.625  $\mu\text{m}$ .

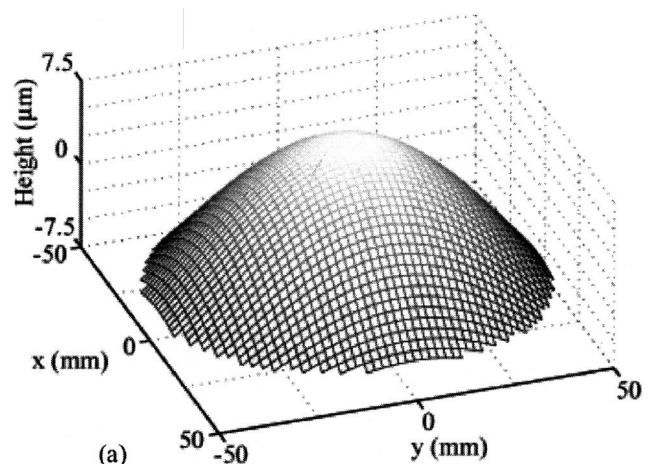
polynomials are a set of orthogonal polynomials within an unit circle.<sup>14</sup> They are defined in cylindrical coordinates as

$$\begin{aligned} \text{even } U_n^l(\rho, \theta) &= R_n^l(\rho)\cos(l\theta), \\ \text{odd } U_n^l(\rho, \theta) &= R_n^l(\rho)\sin(l\theta), \end{aligned} \tag{1}$$

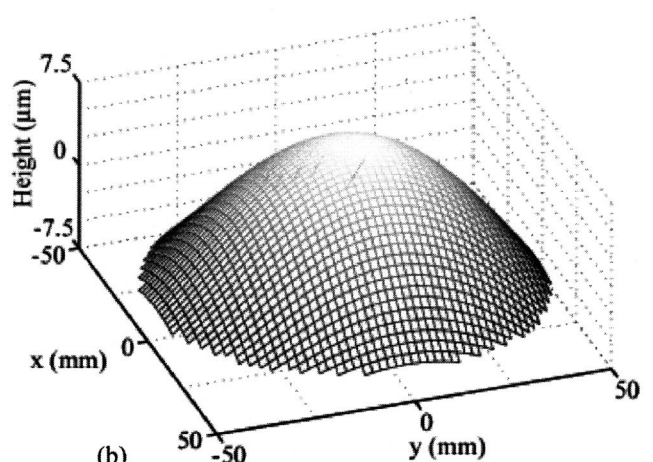
where

$$R_n^{n-2m}(\rho) = \sum_{s=0}^m \frac{(-1)^s(n-s)!}{s!(m-s)!(n-m-s)!} \rho^{n-2s}. \tag{2}$$

Any circular wave front can be expressed as a linear combination of Zernike polynomials due to their orthogonality property



(a)



(b)

FIG. 5. Wafer backsurface profile (a) before, and (b) after the UV-cure imprint process. The peak-to-valley surface topography value changes from 12.910 to 13.145  $\mu\text{m}$ .

$$\begin{aligned} W(\rho, \theta) &= \sum_{n=0}^k \sum_{m=0}^n Z_{nm} R_n^{n-2m} \\ &\times \begin{cases} \sin(n-2m)\theta, & \text{if } n-2m > 0 \\ \cos(n-2m)\theta, & \text{if } n-2m \leq 0 \end{cases} \end{aligned} \tag{3}$$

By comparing the Zernike coefficients, which are the individual weighing terms for each polynomial, single modes of distortion can be analyzed. For small deflection in the linear-elastic regime of the material, out-of-plane distortion induced by thin films is shown to be related only to the change of the  $Z_{21}$  coefficient.<sup>15</sup> Examining the Zernike coefficients as listed in Table I, the changes in the  $Z_{21}$  coefficient are 17 and 28 nm for the thermal-cure and UV-cure process, respectively.

#### IV. RESULTS AND DISCUSSION

For both imprint processes there were a few particle defects, but no release damage was observed over the 100 mm diameter wafer. The blazed facets are well preserved and appear to be identical in both processes, and inverted profiles

TABLE I. Zernike coefficients before and after the thermal-cure and UV-cure imprint processes.

Zernike coefficients ( $\mu\text{m}$ )	Thermal-cure		UV-cure	
	Before	After	Before	After
Z20	0.120	0.032	-0.031	-0.029
Z21	-1.407	-1.39	-6.233	-6.262
Z22	0.023	0.069	-0.209	-0.163
Z30	0.151	0.162	0.087	0.070
Z31	-0.261	-0.234	-0.486	-0.355
Z32	-0.648	-0.659	-0.307	-0.641
Z33	0.057	0.078	-0.004	0.002
Z40	-0.041	-0.052	0.010	0.015
Z41	0.019	0.015	-0.010	-0.000
Z42	0.293	0.286	0.693	0.689
Z43	0.226	0.227	-0.034	-0.026
Z44	-0.165	-0.135	0.015	-0.000

can be seen. There are artifacts in the AFM images caused by the geometric limitations of the probe used. A more accurate profile is illustrated in the SEM image [Fig. 2(b)]. The edge rounding of the imprints is significantly reduced compared to our previous work. However, the exact dimensions are difficult to interpret, since the scanned radius of the edge is close to the radius of the AFM probe ( $\sim 20$  nm).

The rms roughness of the blazed facets is  $<0.2$  nm for both imprint processes. The exact roughness is difficult to estimate since the roughness measurements approached the environmental noise of the AFM, which is around 0.1 nm. The reported rms roughness values are conservative estimates, and we conclude that the replicated gratings show no significant degradation in surface smoothness. The rms roughness values are obtained over spatial frequencies less than 50 nm.

The change of the  $Z_{21}$  coefficient is measured to be around 20–30 nm for both processes. The repeatability of the S–H system is different for each Zernike coefficient, and for  $Z_{21}$  the rms repeatability ( $\sigma_{21}$ ) is around 40 nm. Therefore the change between the measured data is within the measurement repeatability. The out-of-plane distortion induced by the NIL process therefore is less than 40 nm over a 100 mm diameter wafer. This amount of bow is sufficiently small for most applications. The changes of other Zernike coefficients are also on the same order as their respective repeatability. An upper bound estimation for the residual stress based on an out-of-plane distortion of 40 nm is around 10 MPa for the thermal-cure process and 2 MPa for the UV-cure process. The effects of anisotropic grating pattern and polymer thickness variation are small and beyond the resolution of our system.

To evaluate its optical performance, the thermally imprinted blazed grating was tested for x-ray diffraction efficiency. The replicated grating was tested in an off-plane configuration, where the incident x rays are quasiparallel to the grating lines.<sup>16</sup> In this testing geometry the diffracted orders lie on a half cone. The grating was coated with 5 nm of Ti

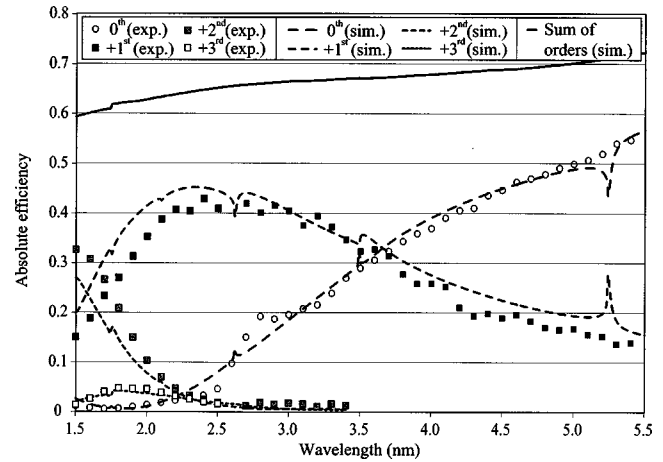


FIG. 6. Preliminary x-ray diffraction efficiencies for the thermally imprinted blazed grating. Experimental data for  $\lambda > 2.5$  nm is taken with a silicon diode detector and properly normalized. Data for shorter wavelengths were taken with an uncalibrated complementary metal-oxide-semiconductor camera. The simulation was done by PCGrate (see Ref. 17) based on an AFM cross-section profile from the metal coated polymer grating.

and 20 nm of Au to increase reflectivity of x rays at grazing incidence. Preliminary results for the absolute x-ray diffraction efficiencies are plotted against incident wavelength, as shown in Fig. 6. The lines are numerical simulations and the points are experimental measurements. The maximum + first order diffraction efficiency is  $\sim 45\%$  at  $\lambda \sim 2.5$  nm. The efficiency is extremely high, as the sum of orders, representing the total reflectivity of the material, is only  $\sim 65\%$  at this wavelength. The x-ray tests were conducted using beamline X24C at the National Synchrotron Light Source of Brookhaven National Laboratory.

## V. CONCLUSION

We have demonstrated high fidelity blazed grating replication using NIL. Using anisotropically etched silicon gratings as the master, we fabricated 200 nm period polymer gratings with  $7.5^\circ$  blaze by imprinting with both the thermal-cure and UV-cure processes onto 100 mm diameter wafers. The replicated gratings show excellent profile conformity and minimal degradation in surface roughness. By analyzing the Zernike coefficients before and after the imprint process, out-of-plane distortion induced by residual stress is shown to be less than 40 nm. An upper bound estimation of residual stress of the imprint film is around 10 MPa. Diffraction efficiency measurements were conducted on the thermally imprinted gratings, and a maximum first order absolute diffraction efficiency  $\sim 45\%$  was observed at  $\lambda \sim 2.5$  nm.

## ACKNOWLEDGMENTS

The authors gratefully acknowledge the outstanding technical assistance of Robert Fleming, Jim Carter, and Jim Daley. Student, staff, and facility support from the Space Nanotechnology Laboratory, NanoStructures Laboratory, and Microsystems Technology Laboratory at MIT are also appreciated. This work was supported by NASA Grant Nos.

NAG5-12583 and NAG5-5405. X-ray data was taken at the National Synchrotron Light Source, Brookhaven National Laboratory, which is supported by the U.S. Department of Energy, Division of Materials Sciences and Division of Chemical Sciences, under Contract No. DE-AC02-98CH10886.

<sup>1</sup>J. V. Bixler, C. J. Hailey, C. W. Mauche, P. F. Teague, R. S. Thoe, S. M. Kahn, and F. B. S. Paerels, *Proc. SPIE* **1549**, 420 (1991).

<sup>2</sup>W. R. Hunter, *Spectrometric Techniques* (Academic, New York, 1985), Vol. IV.

<sup>3</sup>A. E. Franke, M. L. Schattenburg, E. M. Gullikson, J. Cottam, S. M. Kahn, and A. Rasmussen, *J. Vac. Sci. Technol. B* **15**, 2940 (1997).

<sup>4</sup>J. A. Bookbinder, *Proc. SPIE* **4496**, 84 (2002).

<sup>5</sup>N. E. White and H. D. Tananbaum, *Proc. SPIE* **4851**, 293 (2003).

<sup>6</sup>C.-H. Chang *et al.*, *J. Vac. Sci. Technol. B* **21**, 2755 (2003).

<sup>7</sup>S. Y. Chou, P. R. Krauss, and P. J. Renstrom, *Appl. Phys. Lett.* **67**, 3114 (1995).

<sup>8</sup>T. C. Bailey, B. J. Choi, M. Colburn, M. Meissl, S. Shaya, J. G. Ekerdt, S. V. Sreenivasan, and C. G. Willson, *J. Vac. Sci. Technol. B* **18**, 3572 (2000).

<sup>9</sup>A. Rasmussen *et al.*, *Proc. SPIE* **5168**, 248 (2004).

<sup>10</sup>C. R. Forest, C. R. Canizares, D. R. Neal, M. McGuirk, and M. L. Schattenburg, *Opt. Eng.* **43**, 742 (2004).

<sup>11</sup>M. Li, H. Tan, L. Kong, and L. Koecher, *Proc. SPIE* **5374**, 209 (2004).

<sup>12</sup>L. B. Freund and S. Suresh, *Thin Film Materials: Stress, Defect Formation and Surface Evolution* (Cambridge University Press, Cambridge, 2003).

<sup>13</sup>D. R. Neal, W. J. Alford, J. K. Gruetzner, and M. E. Warren, *Proc. SPIE* **2870**, 72 (1996).

<sup>14</sup>D. Malacara, *Optical Shop Testing* (Wiley, New York, 1992).

<sup>15</sup>C.-H. Chang, M.S. thesis, Massachusetts Institute of Technology, 2004.

<sup>16</sup>W. C. Cash, *Appl. Opt.* **30**, 1749 (1991).

<sup>17</sup><http://www.pcgrate.com>.